Molecular Therapy
Oncolytics
Original Article

Expanded NK cells used for adoptive cell therapy maintain diverse clonality and contain long-lived memory-like NK cell populations

David S.J. Allan,[1,4] Chuanfeng Wu,[2,4] Ryland D. Mortlock,[2] Mala Chakraborty,[1] Katayoun Rezvani,[3] Jan K. Davidson-Moncada,[1] Cynthia E. Dunbar,[2,5] and Richard W. Childs[1,5]

[1]Laboratory of Transplantation Immunotherapy, Cellular and Molecular Therapeutics Branch, National Heart Lung and Blood Institute, National Institutes of Health, Bethesda, MD 20892, USA; [2]Translational Stem Cell Biology Branch, National Heart Lung and Blood Institute, National Institutes of Health, Bethesda, MD 20892, USA; [3]Department of Stem Cell Transplantation and Cellular Therapy, University of Texas MD Anderson Cancer Center, Houston, TX 77030, USA

Multiple clinical trials exploring the potential of adoptive natural killer (NK) cell therapy for cancer have employed *ex vivo* expansion using feeder cells to obtain large numbers of NK cells. We have previously utilized the rhesus macaque model to clonally track the NK cell progeny of barcode-transduced CD34$^+$ stem and progenitor cells after transplant. In this study, NK cells from barcoded rhesus macaques were used to study the changes in NK cell clonal patterns that occurred during *ex vivo* expansion using culture protocols similar to those employed in clinical preparation of human NK cells including irradiated lymphoblastoid cell line (LCL) feeder cells or K562 cells expressing 4-1BBL and membrane-bound interleukin-21 (IL-21). NK expansion cultures resulted in the proliferation of clonally diverse NK cells, which, at day 14 harvest, contained greater than 50% of the starting barcode repertoire. Diversity as measured by Shannon index was maintained after culture. With both LCL and K562 feeders, proliferation of long-lived putative memory-like NK cell clones was observed, with these clones continuing to constitute a mean of 31% of the total repertoire of expanded cells. These experiments provide insight into the clonal makeup of expanded NK cell clinical products.

INTRODUCTION

Natural killer (NK) cells exhibit spontaneous cytotoxicity toward tumor cells, with a growing number of immunotherapeutic trials being developed to test the anti-tumor potential of these populations in the clinic.[1,2] Notably, select trials have established that the adoptive infusion of cytokine-activated allogeneic NK cells after lymphodepleting chemotherapy can result in complete remissions (CRs) in one-quarter to one-half of patients with acute myeloid leukemia (AML).[3–7] Cancer therapies have also sought to utilize NK cells' potent mediation of antibody-dependent cell-mediated cytotoxicity (ADCC) via concurrent administration of NK cells with monoclonal antibodies.[8–10]

NK cells typically constitute only 2%–20% of peripheral blood lymphocytes, restricting the frequency of administration and number of NK cells that can be infused following isolation by leukapheresis. To facilitate larger doses, to forgo the need for repeated leukapheresis, or to allow multiple individuals to be treated with the same product, expansion of NK cell numbers in culture has been explored. Feeder-free cultures containing interleukin-2 (IL-2) or IL-15 cytokines alone increase NK cell numbers by only a few fold.[11–13] Early studies showed that interaction with irradiated Epstein-Barr virus (EBV)-transformed lymphoblastoid cell lines (LCLs) triggered proliferation of NK cells,[14] with this effect being amplified by simultaneous exposure to IL-2.[15,16] Our research group developed a good manufacturing practice (GMP)-compliant method to expand large numbers of highly purified populations of clinical-grade NK cells (FDA IND 13663) through co-culture with irradiated LCL feeder cells and IL-2: NK cells produced by these cultures expanded a mean 490-fold over 21 days, with increased TRAIL (TNFSF10) surface expression, higher levels of cytokine production, and greater tumor cytotoxicity compared with non-expanded NK cells.[17] Infusion of up to 5×10^8 NK cells/kg was shown to be safe and well tolerated in patients with advanced malignancies who were pre-treated with bortezomib to sensitize tumors to TRAIL-mediated NK cell killing.[18,19]

The NK-cell-sensitive leukemic cell line K562, modified to express 4-1BBL (TNFSF9/CD137L) and surface-bound IL-15[13,20] or surface IL-21,[21] also triggered profound expansion of NK cell numbers in *ex vivo* co-cultures. Changes in the phenotypic, functional, and transcriptional aspects of NK cells expanded using either LCL cells or

Received 2 June 2022; accepted 23 December 2022;
https://doi.org/10.1016/j.omto.2022.12.006.

[4]These authors contributed equally

[5]These authors contributed equally

Correspondence: Cynthia E. Dunbar, Translational Stem Cell Biology Branch, National Heart Lung and Blood Institute, National Institutes of Health, 10 Center Drive, Bethesda, MD, 20892, USA.
E-mail: dunbarc@nhlbi.nih.gov
Correspondence: Richard W. Childs, Laboratory of Transplantation Immunotherapy, Cellular and Molecular Therapeutics Branch, National Heart Lung and Blood Institute, National Institutes of Health, 10 Center Drive, Bethesda, MD, 20892, USA.
E-mail: childsr@nhlbi.nih.gov

K562 cells have been well characterized and appear similar.[13,17,21–23] NK cell products generated using K562 feeder cells have been employed in multiple small clinical trials in individuals with AML, myelodysplastic syndrome, chronic lymphocytic leukemia,[24–27] medulloblastoma, ependymoma,[28] multiple myeloma,[29,30] and solid tumors[31] in different regimens including combinations with other agents, after chemotherapy, or post-stem cell transplant. Stimulation of NK cells by K562- or LCL-based feeder cells are also utilized in protocols as a key component to enhance viral transduction to generate NK cells bearing transgenes such chimeric antigen receptors (CARs) or growth receptors.[20,32–35] Strikingly, in a recent clinical trial, patients with non-Hodgkin's lymphoma or chronic lymphocytic leukemia receiving expanded NK cells expressing an anti-CD19 CAR and IL-15 showed CR in 7 of 11 cases.[33]

To date, analysis of the clonal composition of NK cells following expansion has remained a challenge, with relevance to questions such as whether all NK cells have expansion potential or whether a small specific subclass of NK cells or precursors are responsible for expanded NK cell numbers. Such an analysis is more difficult with NK cells compared with T cells or B cells as clonal tracking of rearranged gene segments such as T cell receptor (TCR) or B cell receptor (BCR) cannot be performed. As a result of stochastic expression of receptors during cell development, NK cells do exhibit a complex repertoire of receptor combinations on individual circulating cells, perhaps evolved, in part, to recognize mutations in cancer cells, such as loss of single major histocompatibility complex (MHC) alleles.[36] Further diversity is afforded by NK cell education, pathogen experience, and tissue microenvironment. High-dimensional flow or mass cytometry has been used to survey NK cell receptor combinations *ex vivo*,[37,38] but these cannot uniformly resolve individual NK cell clones arising by proliferation from single NK cells or progenitors. Although clinical correlations are advancing, it is presently unclear which elements of the NK cell repertoire are key in mediating the anti-tumor effects observed in clinical adoptive NK cell therapy trials. In T cells, selected studies examining the TCR repertoire before and after antigen-specific or antibody-driven expansion have revealed significant *in vitro* alterations, including repertoire skewing and changes to immunodominant clones[39,40] that may be of clinical relevance. Therefore, deciphering changes that occur in clonal architecture associated with commonly used expansion protocols could enhance our understanding of the impact of *ex vivo* NK cell expansion on the immunotherapeutic potential of these immune effectors.

Our laboratory has utilized the rhesus macaque model to clonally track the hematopoietic progeny of transplanted $CD34^+$ stem and progenitor cells that have been transduced with "barcoded" lentiviral vector libraries. Investigation of NK cells in these transplanted animals revealed large NK cell clones that were significantly expanded or unique compared with other cell lineages.[41,42] Cells of each barcoded NK cell clone were often uniformly positive or negative for expression of a given killer immunoglobulin-like receptor (KIR), suggesting origination of the clones from single NK cells that had already fixed their KIR expression.[41] Importantly, expanded macaque NK clones persisted for multiple years and waxed and waned in possible response to environmental stimuli.[41] Individual animals were heterogeneous in terms of numbers and total frequency of expanded NK clones observed. Appearance of new groups of expanded NK clones was observed after infection with rhesus cytomegalovirus (CMV).[43] The long-lived clonal nature suggests a close relationship with the phenomenon of NK cell memory wherein NK cells exhibit enhanced recall responses to specific viruses or chemicals.[44] Features of memory-like NK cells, including enhanced antibody-dependent effector potential and capacity to persist *in vivo* may make these cells particularly suited to mediate long-lasting anti-cancer immunotherapeutic effects.

In this study, NK cells from barcoded macaques were used in experiments to illuminate the impact of *ex vivo* expansion on the clonal repertoire of NK cell populations, focusing on protocols that incorporate feeder cells and culture conditions typical of the numerous human clinical trials mentioned above. Changing contributions of putative memory-like NK cells to the repertoire of this immunotherapeutic population was also explored.

RESULTS

Expansion of NK cells with irradiated LCL feeder cells results in proliferation of a diverse clonal repertoire

To study the clonal patterns of NK cells undergoing *ex vivo* expansion, we examined rhesus macaques that had previously undergone autologous transplantation with barcoded hematopoietic stem and progenitor cells (HSPCs). Animals received conditioning with ablative total-body irradiation followed by infusion of $CD34^+$ HSPCs transduced with lentiviral vectors encoding CopGFP and a high-diversity library of 27 or 35 bp random barcode DNA sequences. Barcode DNA sequences could be tracked in various hematopoietic lineages over extended periods following transplantation and revealed marked oligoclonal, KIR-specific expansions of $CD16^+$ NK cell clones.[41,42] At the time of the current study, the animals showed stable hematopoietic engraftment (41–76 months after transplantation).

Purified peripheral blood $NKG2^+$ ($KLRC1^+$ or/and $KLRC2^+$) $CD3^-$ $CD20^-$ $CD14^-$ NK cells were isolated from barcoded animals and queried by PCR and next-generation sequencing to determine the clonal repertoire of barcodes. A fraction of concurrently isolated NK cells was subjected to *ex vivo* expansion by co-culture with irradiated LCL feeder cells and IL-2 (Figure 1A) as previously reported and utilized in a clinical trial (ClinicalTrials.gov: NCT00720785).[17,18] Rhesus NK cell numbers expanded efficiently under these conditions. At various time points in culture, aliquots of cells were removed for barcode retrieval and longitudinal comparisons with the starting clonal repertoire, as shown in heatmaps depicting individual clonal abundances focusing on the most abundant clones (Figure 1B). Clones showed a variety of patterns of behavior upon culture, some increasing or decreasing in frequency or remaining stable over time. None of the most abundant clones disappeared completely from culture over time (dark blue in Figure 1B). Notably, measures of the Shannon index, an established measure of clonal diversity,[45] were

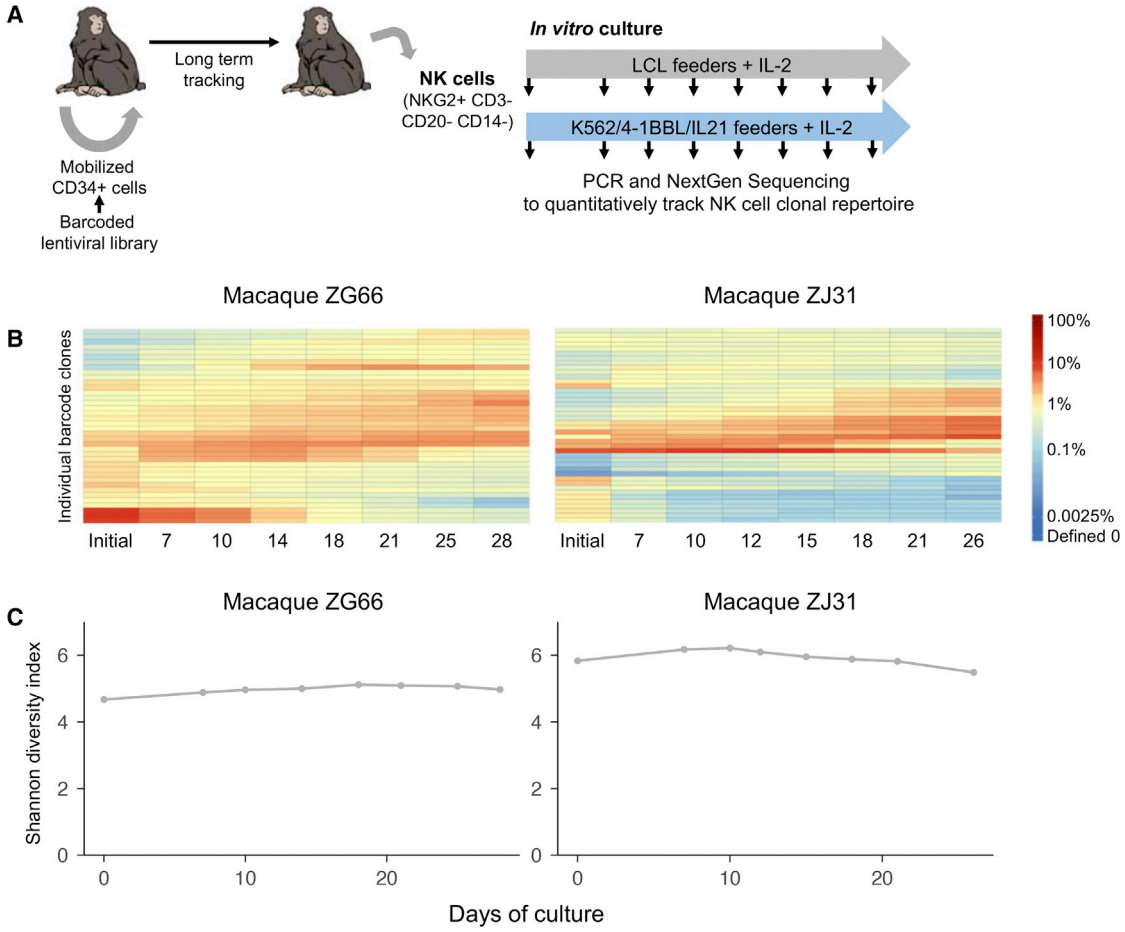

Figure 1. Rhesus macaque NK cells cultured with LCL feeder cells and IL-2 maintain clonal diversity

(A) Experimental design: rhesus macaques previously underwent autologous hematopoietic stem cell transplantation with purified $CD34^+$ cells marked by lentiviral barcodes following ablative total body irradiation. $NKG2^+$ $CD3^-$ NK cells from these macaques were fluorescence-activated cell sorted and cultured *in vitro* with irradiated human LCL cells and 500 U/mL IL-2 (or in additional experiments detailed below with K562 feeder cells). The barcode repertoire was sampled by PCR and next-generation sequencing initially and at the indicated days of culture. (B) Heatmap of clonal frequency of the most abundant clones throughout culture. Clones registering among the 20 most frequent at any time point are shown. Each row is a barcode, each column is a sample, and the color scale shows the barcode frequency. (C) Shannon diversity index of barcode frequencies.

very consistent over time, reflecting continued diversity of the NK cell repertoire (Figure 1C).

The wider clonal repertoire in NK cells was analyzed in another way. Clones were included in analysis if they contributed above a frequency threshold approximating the equivalent of 1 cell amid the cells sampled for PCR at the start of culture. This allowed tracking of 682 clones in culture of NK cells from animal ZG66 and 3523 clones from ZJ31. Strikingly, 62%–71% of initial barcodes were detected in cultured ZG66 cells at subsequent time points (Figure 2A). In cultured ZJ31 cells, 53% of initial barcodes could be identified after 15 days, although percentages lessened with increasing duration (Figure 2A). Undetected clones may have disappeared from culture or may have fallen below the frequency of detection of the PCR/sequencing assay. To gauge occurrence of the latter, the frequency of clones that became undetectable at a given time point but were again detected later in culture were tabulated (Figure 2A). Decreasing the detection threshold by an order of magnitude when analyzing samples that were in culture for 14–15 days also boosted the proportion of detected clones to 72% (ZG66) or 62% (ZJ31) (data not shown).

Changes in clonal frequency were studied throughout the culture period. Each individual clone's contribution was normalized to initial frequency, and the distribution of these values depicted as a scatter/violin plot (Figure 2B). Focusing on clones that continued to be detected, Figure 2C summarizes the same data in box plots, with whiskers representing the 10^{th} and 90^{th} percentiles. This analysis revealed a surprising stability in clonal frequencies. Despite the overall cell numbers in culture increasing by 300- to 450-fold by culture days

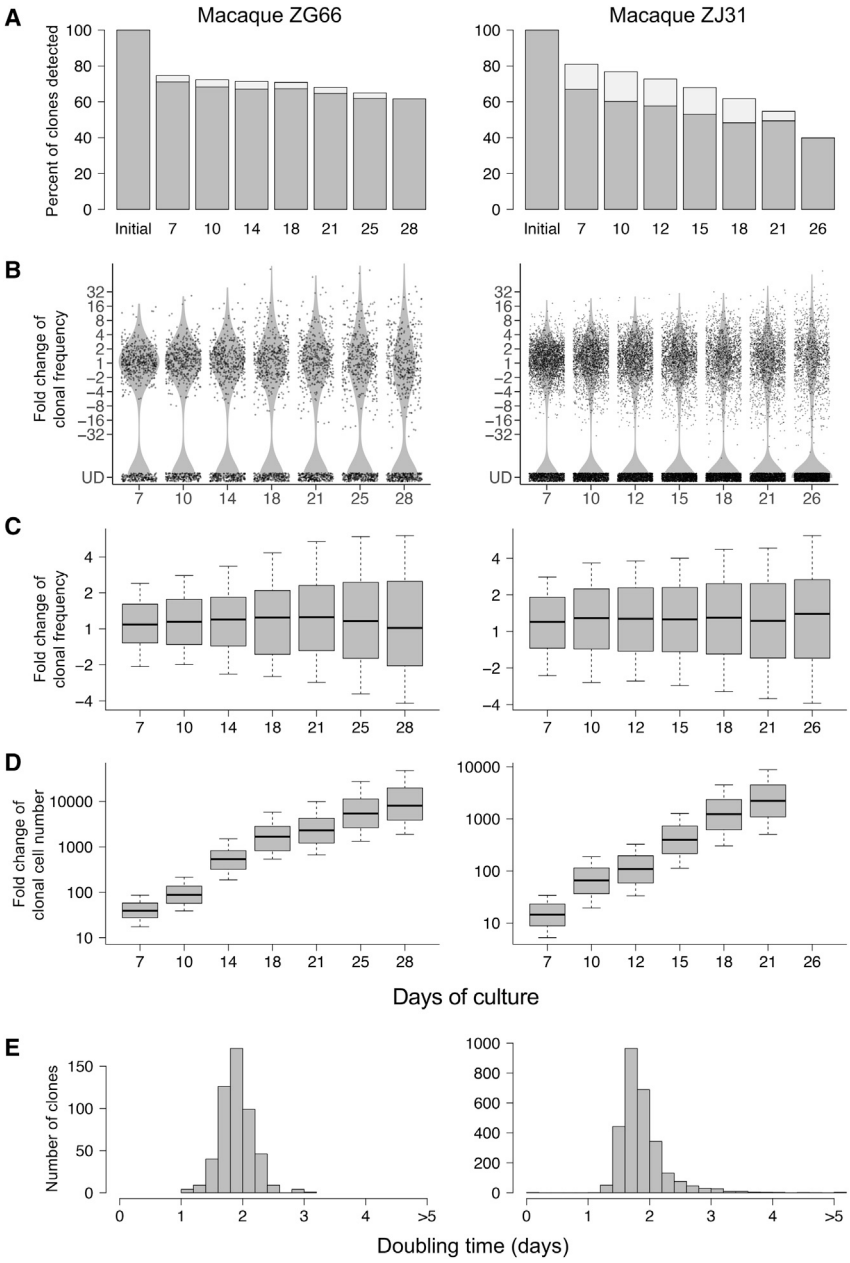

Figure 2. *In vitro* cultures of rhesus macaque NK cells with LCL feeder cells and IL-2 demonstrate proliferation of the majority of barcoded clones

Analyses of all clones having a frequency greater than the estimated equivalent of 1 cell amid the initially sampled population, allowing tracking of 682 barcodes and 3,523 barcodes for animals ZG66 and ZJ31, respectively, from the same experiments shown in Figure 1. (A) Percentage of initial barcodes that were subsequently detected at each time of culture (gray bars) or undetected/below threshold at a given time point but detected at a later instance during culture (light gray bars). (B) Distribution of clonal frequencies over time, normalized to initial frequency in NK cells. Calculated as barcode frequency divided by the frequency at the start of culture (UD, undetected or below threshold). (Values <1 are depicted as negative reciprocal.) (C) Boxplot representation of data from (B) showing median and quartiles of detected clones, with whiskers showing 10th and 90th percentiles of measures. (D) Distribution of estimates of clonal fold expansion in cell number, calculated by multiplying the fold change in clonal frequency for each clone (as in C) with the overall expansion in cultured NK cell number measured by cell counting. (E) Distribution of clonal doubling times determined by fitting a model of exponential growth for each clone across the interval shown. (C)–(E) show clones above the detection threshold at the indicated time points, corresponding to gray bars in (A). Similar analyses of expansion cultures of NK cells from animals ZK22 and ZH19 are shown in Figure S1.

14–15, more than 80% of clones remained within 4-fold of their initial frequencies in both animals (Figure 2C). The spread of the distribution increased with time, presumably reflecting the increasing opportunity to diverge in frequency upon continued cell division (Figure 2C).

To estimate the proliferation of individual clones, the fold expansion in overall cell number was multiplied by the fold change in frequency for each barcode (Figure 2D). This revealed a distribution of clones that increased in cell number in expansion cultures over time (Figure 2D). Fitting a model of exponential growth across all time points for each clone allowed estimation of the distribution of doubling times of detected clones (Figure 2E). Similar results were observed in shorter-duration cultures from two additional animals (Figure S1). Overall, these results support the conclusion that these *in vitro* expansion culture conditions using irradiated LCL feeder cells and IL-2 promote proliferation of a diverse repertoire of clones.

Similar clonal patterns in NK cells expanded with irradiated LCL and K562 feeder cells

Several centers have utilized a K562 cell line transfected with 4-1BBL and cytokines for the *ex vivo* expansion of clinical grade NK cells,[24–31] including NK cells transduced to express CARs.[33] Therefore, we compared the clonal repertoire of rhesus NK cells expanded with irradiated LCL feeder cells with those expanded with irradiated K562/4-1BBL/IL-21 cells. These experiments revealed comparable changes in Shannon diversity index in most cases (Figure 3A) and similar percentages of detected clones during culture (Figure 3B). Among detected clones, the distributions of clonal change in frequency after 14–15 days appeared similar when stimulated with either feeder cell type (Figures 3C and S2A), but the estimates of the overall fold change in clonal cell numbers trended to be higher with K562/4-1BBL/IL-21 than with LCL feeders (Figures 3D and S2B). The effects associated with repeating feeder cell stimulation were also investigated. Cultures

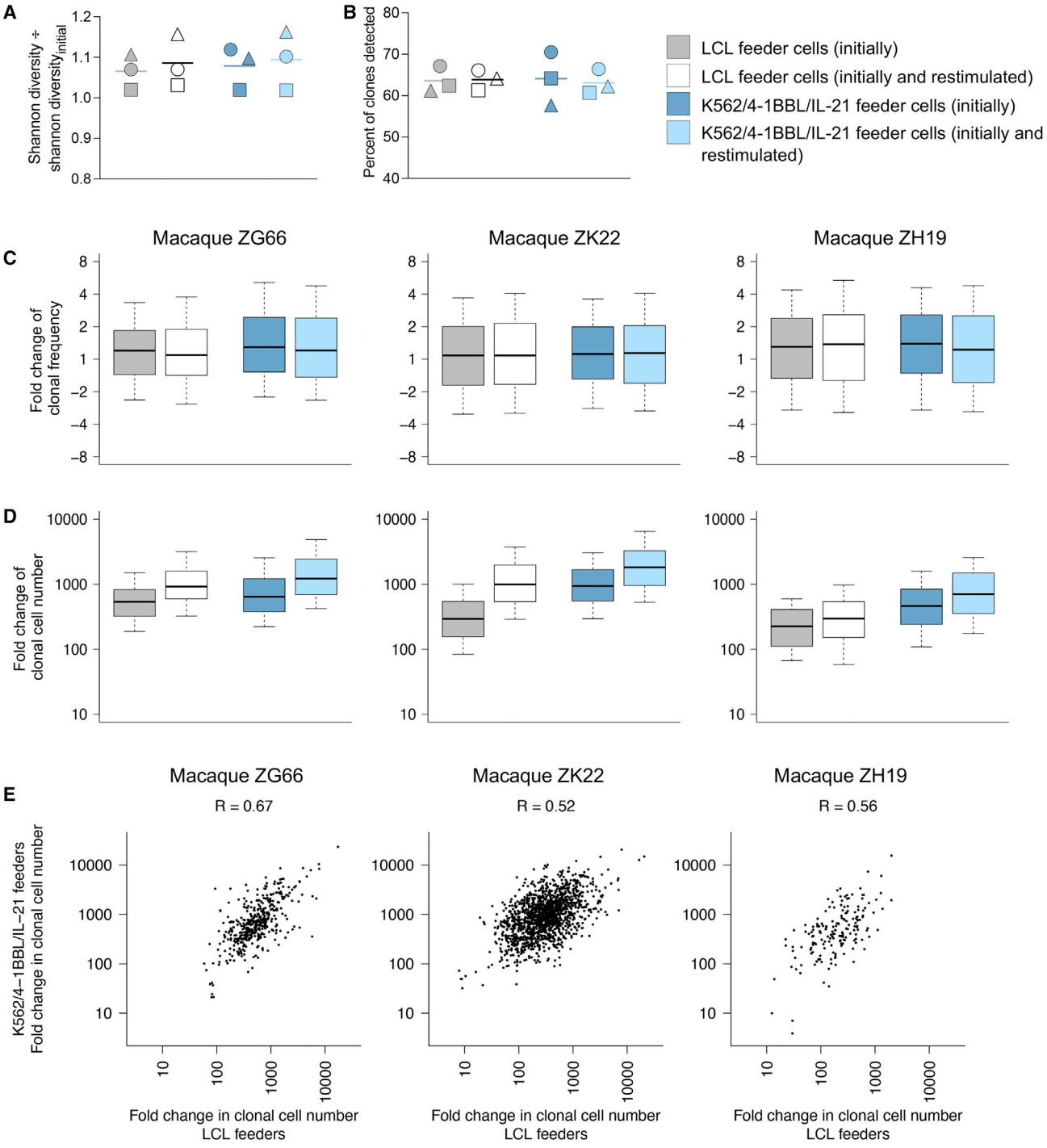

Figure 3. Similar effects on clonal repertoire in NK cells expanded with irradiated LCL and K562/4-1BBL/IL-21 feeder cells

(A–D) The cultures of barcoded macaque NK cells initiated with irradiated LCL feeder cells as described in Figures 1 and 2 (gray) are contrasted with NK cell cultures initiated with irradiated K562 cells expressing 4-1BBL and IL-21 (dark blue) in both cases, with feeder cells added only at the start of culture. NK cell cultures started identically but restimulated by readdition of irradiated feeder cells approximately weekly are shown for comparison (white and light blue). (A) Shannon diversity index of barcodes at day 14–15 of culture divided by the Shannon index of the starting NK cell population (circles, macaque ZG66; squares, ZK22; triangles, ZH19). (B) Percentage of initial barcodes that were above detection threshold on day 14–15. (C) Distribution of clones' frequency at day 14–15 of culture, normalized to initial frequency in NK cells. (D) Distribution of the fold expansion of clones in cell number at day 14–15, calculated as indicated in Figure 2. Boxplots represent median and quartiles, while whiskers show 10th and 90th

(legend continued on next page)

restimulated by weekly addition of irradiated feeders showed slightly higher measures of the spread of the distribution of clonal frequency change compared with cultures receiving irradiated feeder cells only at the initiation of culture (Figure S2A).

Paired NK cultures stimulated with LCL and K562/4-1BBL/IL-21 feeder cells provided the opportunity to determine if individual clones had reproducible behavior under these two conditions. As shown in Figure 3E, the fold change in cell number in various clones expanded in LCL cultures showed considerable correlation with cultures stimulated with K562/4-1BBL/IL-21. Pearson correlation coefficients were 0.67, 0.52, and 0.56 in cultures from animals ZG66, ZK22, and ZH19, respectively. This implies that clones exhibit certain inherent features that make them more or less likely to proliferate in either of these culture systems.

NK cell clones pre-expanded *in vivo* show lesser subsequent *in vitro* proliferation but continue to constitute a significant proportion of the repertoire

To identify clonal characteristics that correlate with any observed differences in clonal proliferative capacity in culture, clones were classified based on additional information. We have previously observed that certain NK clones are expanded during development *in vivo*, compared with frequencies of the same barcode in other hematopoietic lineages, resulting from presumptive pathogen-driven or homeostatic processes.[41,42] On the other hand, classical monocytes have a short half-life in blood, being continually replenished from progenitor cells,[46] and their barcode repertoire closely resembles that of HSPCs. By comparing with barcode frequency in monocytes isolated concurrently, barcodes detected in NK cells were statistically categorized into those which were expanded *in vivo* relative to monocytes ($p < 0.05$ by chi-squared test) and contrasted with other clones that did not fit this criterion ($p > 0.05$). Comparison between animals revealed different contributions of *in vivo* expanded clones to the repertoire at the start of culture, perhaps reflecting different immune and infection history of the animals (although the numbers of cells sorted in each experimental population also played a role in statistically defining the subsets). Interestingly, clones categorized as pre-expanded in NK cells *in vivo* nevertheless exhibited considerable subsequent proliferation *in vitro* using these culture systems, with the majority expanding 30- to 1,100-fold in number by day 14–15 (Figure 4A). However, the proliferation in culture of these *in vivo* expanded clones was less than clones that were not designated as being as expanded *in vivo* ($p < 0.05$ by t test in 6 of 7 comparisons performed) (Figure 4A), possibly implying that some degree of reduced potential or proliferative exhaustion had occurred in the former population. By summing the frequencies of clones within each category, the proportion to which pre-expanded NK cells contribute to the overall NK cell repertoire throughout the expansion culture is estimated in Figure 4B. Similar results are obtained if categorizing these clones with even more stringent criteria (Figure S3).

Large expanded NK clones can persist many months *in vivo* independent of continued maturation and replenishment from bone marrow stem and progenitor cells,[41] providing evidence that these populations are related to memory-like, adaptive, or trained NK cell immunity,[44,47,48] possibly dependent on ongoing stimulation *in vivo* over time. The vast majority of these clones had a mature $CD16^+$ phenotype.[42] It is noteworthy that the animals included in this study are all rhesus CMV seropositive and naturally infected early in life with CMV and likely a spectrum of other viruses. To consider the element of persistence when segregating clones, an alternative analysis was performed: persistent expanded clones were classified as those expanded in $CD16^+$ NK cells relative to monocytes both at the initiation of culture and independently in a blood draw from the same animal 8–12 months previously (both $p < 0.05$ by chi-squared test). Persistent expanded clones were still able to proliferate *in vitro* upon co-culture with irradiated feeder cells but less so than other clonal populations that had undergone less *in vivo* expansion (Figure 4C). The summed frequency of contributions to the overall NK cell repertoire by these *in vivo* persistently expanded clones is shown in Figure 4D. In summary, *in vivo* pre-expanded memory-like or persistently stimulated NK cell clones continued to represent a significant fraction of the generated NK cell product.

Clones were also categorized based on expression of KIR. Previous studies documented segregation of individual clones with expression of specific KIR.[41] Anti-KIR monoclonal antibody NKVFS1 shows reactivity with rhesus NK cells bearing the Mamu-KIR3DL01 gene product.[49] NK cells positive and negative for binding to NKVFS1 were sorted from animals and profiled by PCR and sequencing to determine the respective barcode repertoires. This facilitated statistical categorization of clones as predominantly $KIR3DL01^+$, primarily $KIR3DL01^-$ (based on 90% confidence of 5-fold higher frequency in the sorted subset), or other clones (either comprised of mixed $KIR3DL01^+$ and $KIR3DL01^-$ cells or having too few sequencing reads to classify with confidence). The contributions of clones in these categories to the overall NK repertoire throughout culture is shown in Figure 5. Clones positive for this KIR persisted throughout culture with no clear preferential loss or expansion. The rhesus macaque KIR3DL01 receptor recognizes macaque Bw4 MHC alleles Mamu-B*007:01, -B*041:01, -B*058:02, and -B*065:01;[49] however, it is unclear if this receptor would bind human MHC expressed by the LCL line.[50] In prior flow cytometry studies, proportions of human NK cells expressing KIR tended to decrease during expansion with irradiated LCL feeders.[51] Highly biased expression of KIR in barcoded macaque clones provides compelling evidence for origin of those clones from single NK cells expressing or lacking KIR, followed by expansion

percentiles of clonal measures. (E) Scatterplot of day 14–15 clonal fold expansions in cell number showing paired cultures stimulated initially with either feeder cell line. Each dot represents a barcode. Only barcodes detected in both samples are shown. Pearson correlation coefficient is also displayed. Results using cells from three transplanted macaques are shown as indicated. Comparisons of feeder cells and restimulation conditions were not performed using NK cells from animal ZJ31. One clone in blood of animal ZH19, present in bulk samples but detected much less in GFP^+ sorted samples, was excluded from analyses in (A)–(C) because groups differed in sorting status.

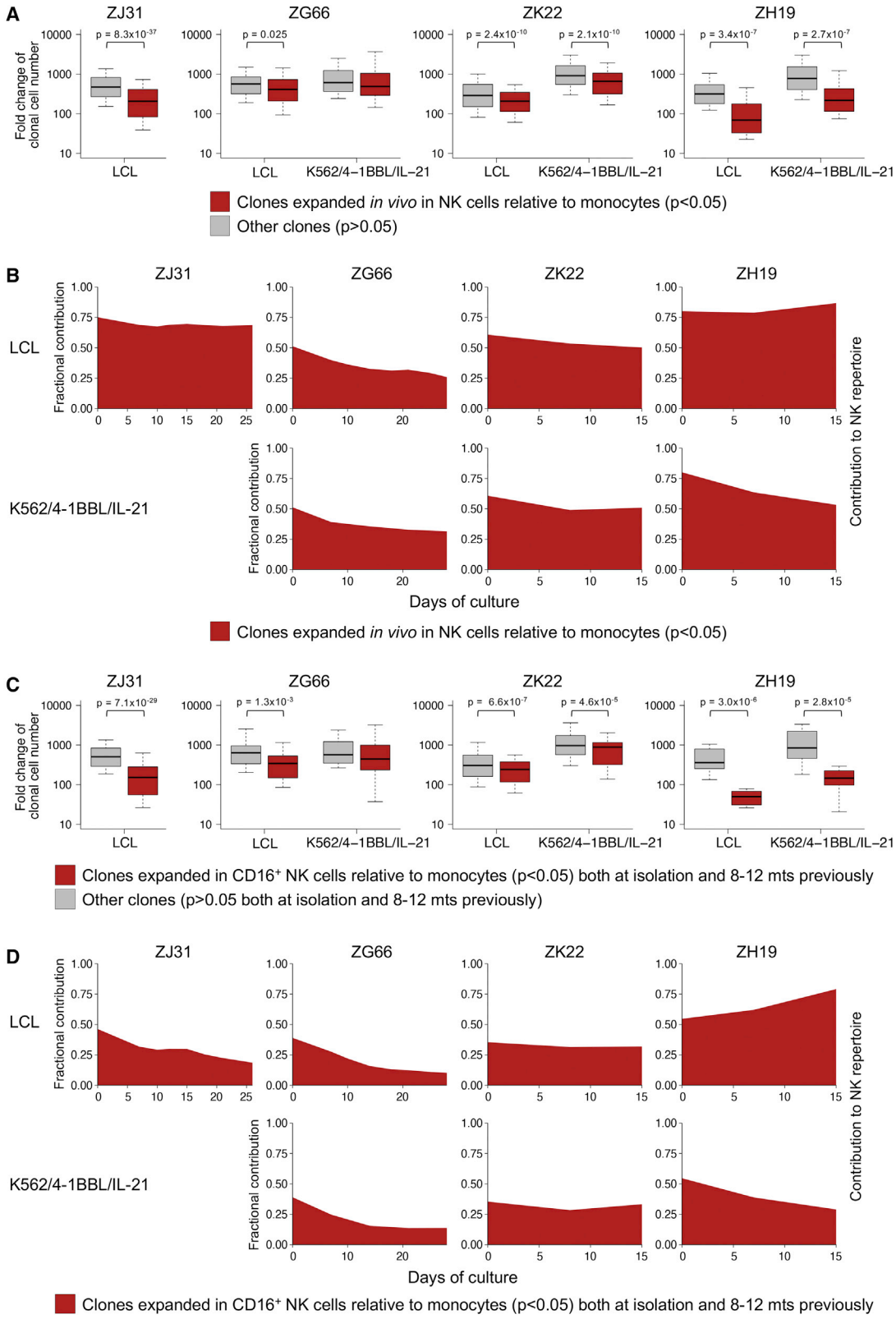

(legend on next page)

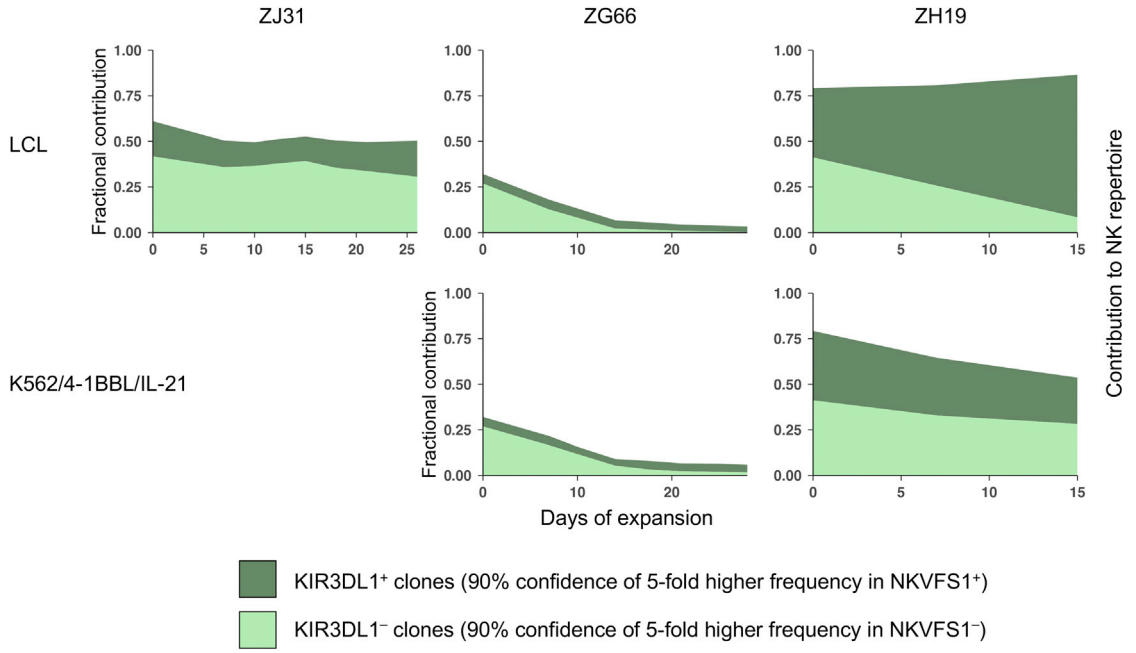

Figure 5. NK cell clones with specific KIR expression expand *in vitro*

At or near the same time as initiating *in vitro* cultures, blood NKG2$^+$ CD3$^-$ NK cells were sorted into positive and negative subsets for binding the NKVFS1 antibody, which recognizes rhesus macaque KIR3DL01. Barcodes were profiled by PCR and next-generation sequencing. Inferring the number of sampled cells bearing each barcode allowed estimation of confidence intervals for relative barcode abundance between the populations (see materials and methods). This permitted categorization of barcode clones as predominantly KIR3DL01$^+$ (having 90% confidence that frequency is 5-fold higher in sorted NKVFS1$^+$ cells) (dark green) or predominantly KIR3DL01$^-$ (having 90% confidence that frequency is 5-fold higher in sorted NKVFS1$^-$ cells) (light green) or all other barcodes that do not meet these stringent criteria for KIR3DL01 bias (white). Contribution of barcodes with these categorizations to the overall NK cell repertoire throughout the duration of *in vitro* culture are shown. Cultures are as described in Figures 1, 2, and 3, stimulated with the indicated feeder cell line only initially, except for ZH19 cultures, which were also restimulated after approximately 1 week. NK cells from ZK22 did not show reactivity with antibody NKVFS1, presumably due to KIR polymorphism, precluding similar analysis from this animal.

in vivo while retaining KIR status, then continued contribution *in vitro* of these clones to the NK cell product generated. Consistent with this theory, contributions of different animals' highly KIR3DL01 biased (positive plus negative) clones to the repertoire (Figure 5) mirrored the contributions of *in vivo* expanded NK clones categorized independently in Figure 4.

Both CD56 NK-cell-biased and CD16 NK-cell-biased clones expand *in vitro*

Rhesus macaque NK cells include CD56$^+$ and CD16$^+$ subsets (Figure 6A) having phenotypic, functional, and transcriptomic similarities with human CD56^{bright} and CD56^{dim} CD16$^+$ subsets, respectively (Webster and Johnson[52] and S. Cordes, C.W., and C.E.D., unpublished data). Human CD56^{bright} NK cells show much more proliferation in response to IL-2 or IL-15 stimulation compared with CD56^{dim} cells.[12] Macaque CD56$^+$ or CD16$^+$ NK subsets were sorted concurrently (or close to the initiation of culture) and profiled for barcode repertoires. As above, clones present in the bulk NK cell population could be classified as biased to a higher frequency in the CD16$^+$ subset or biased to be more abundant in CD56$^+$ NK cells ($p < 0.05$ by chi-squared test). Both clone categories continued to contribute to the overall NK repertoire throughout NK cell culture with irradiated feeders, although initially, CD16$^+$ NK-cell-biased clones decreased somewhat in collective frequency in some cases (Figure 6B). In

Figure 4. NK cell clones previously expanded *in vivo* maintain the capacity to subsequently proliferate *in vitro*

(A and B) Barcode clones present in NK cells at the start of culture were compared with their frequency in sorted monocytes isolated at the same time. Inferred numbers of sampled cells bearing each barcode were compared between populations by chi-squared test, allowing categorization of clones pre-expanded *in vivo* in NK cells relative to monocytes ($p < 0.05$) and other clones ($p > 0.05$). These groupings of barcodes were then followed through *in vitro* culture with irradiated feeder cells and IL-2. (A) Distribution of the fold expansion of clones in cell number at day 14–15 *in vitro* is shown. Differences between clone categories were examined by t test, generating the depicted p values. (B) Estimation of the contribution of *in vivo* pre-expanded clones to the overall NK cell repertoire throughout *in vitro* culture. The barcode frequencies of clones within the indicated category were summed at each time point analyzed. (C and D) Similar analyses of expanded NK clones adding the constraint that clones are persistently expanded *in vivo* (categorized as higher in CD16$^+$ NK cells relative to monocytes both at the initiation of culture and independently in blood 8–12 months earlier from the same animal [$p < 0.05$ by chi-squared test at both time points]) versus other clones ($p > 0.05$ at both instances). The cultures shown in (A)–(D) were stimulated with the indicated irradiated feeder cell line only initially, except for ZH19 cultures, which were also restimulated after approximately 1 week. Boxplots show median, quartiles, 10th, and 90th percentiles.

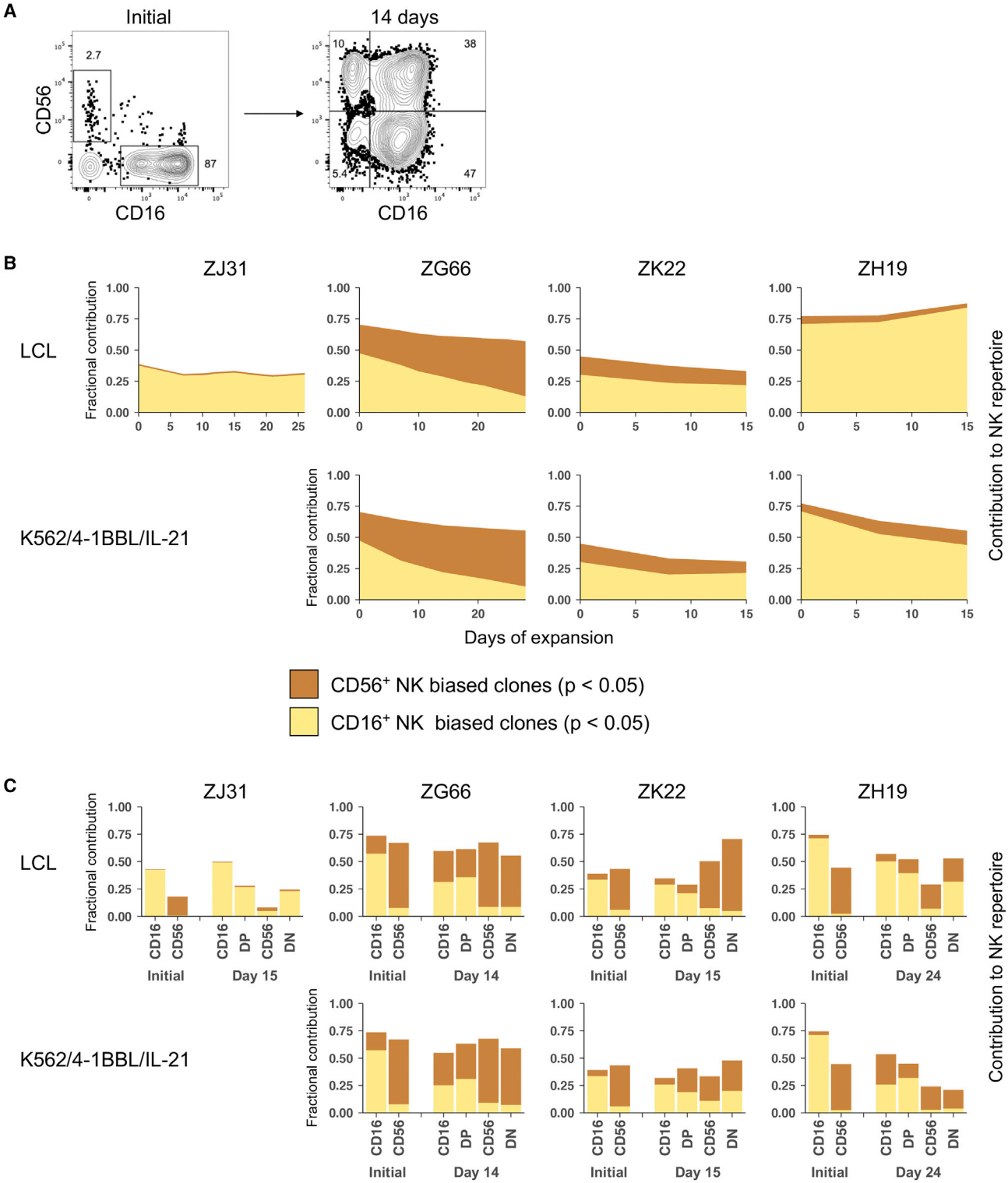

Figure 6. Both CD56 NK-cell-biased and CD16 NK-cell-biased clones expand *in vitro*

Blood CD56$^+$ and CD16$^+$ NK cell populations were flow-cytometry sorted from the same animals at or near the time of initiating *in vitro* NK cell cultures, then examined by barcode PCR and sequencing. Comparing inferred numbers of sampled cells bearing each barcode by chi-squared test allowed categorization of clones biased to higher

(legend continued on next page)

resulting cells after >14 days of culture, multiple subsets of cells could be defined by these markers (Figure 6A) and were sorted and queried for barcodes. Clones that had been classified as biased toward the $CD16^+$ NK cell population at the initiation of culture contributed most in frequency to the $CD16^+$ $CD56^-$ and $CD56^+$ $CD16^+$ populations after culture (Figure 6C). Conversely, clones starting as $CD56^+$ biased constituted more of the resulting $CD56^+$ $CD16^-$ and $CD56^-$ $CD16^-$ subsets (Figure 6C). This was consistent with the predominant phenotypes of expansion cultures initiated with isolated $CD16^+$ or $CD56^+$ rhesus NK cells and LCL performed earlier from animals ZG66 and ZH19 (Davidson-Moncada et al.[53] and data not shown). The human analog of the macaque blood $CD56^-$ $CD16^-$ NK cell subset is less clear; however, an analysis incorporating clones biased to this initial subset is shown in Figure S4. Subset clonal repertoires were also compared by Pearson correlation before and after expansion, with similar findings. On average, the barcode repertoire of initially $CD16^+$ NK cells correlated most with $CD16^+$ and $CD16^+$ $CD56^+$ subsets after bulk culture of the NK cells (Figure S5). These results indicate some phenotypic plasticity of biased clones upon extensive proliferation *in vitro*, especially in expression of the rhesus macaque CD56 receptor. However, both initially $CD56^+$ NK-cell-biased and especially $CD16^+$ NK-cell-biased clones contributed significantly to the resultant expanded NK cell products.

DISCUSSION

Rhesus macaques bearing a barcoded hematopoietic system were employed to examine clonal dynamics during *ex vivo* NK cell expansion cultures. Previously, NK cells expanded using these protocols for human NK cell immunotherapy trials were characterized by flow cytometry staining, functional assays, and transcriptomics. However, the clonal architecture of these cell products could only be inferred given the lack of clonal receptor rearrangements in most NK cells in contrast to T cells or B cells, where TCR or BCR gene rearrangements facilitate clonal tracking. Our studies revealed several intriguing findings. First, the majority of clones identified in rhesus NK cells upon isolation continued to be detected in culture following *ex vivo* expansion with irradiated feeder cells. Furthermore, many clones remained within approximately 4-fold of their original frequency despite huge increases in the overall cell numbers of expanded NK cells (averaging 625-fold at day 14) (Figure 2). These results would appear to contrast with certain studies of T cells that revealed considerable changes to the TCR clonal repertoire upon antigen-specific or antibody-driven expansions in cell number for immunotherapy.[39,40]

When interpreting these results, it is important to consider what individual barcodes represent. Animals were transplanted with $CD34^+$ HSPCs transduced with a library of barcode vectors, not with NK cells. Therefore, a barcode should mark the progeny of a given HSPC. Many stem cells continually generate cells of multiple lineages including NK cells. Given this ongoing production, and the stochastic acquisition of NK receptors during development, some barcodes likely encompass within the NK compartment a "family" of multiple NK cell specificities derived from a single HSPC. These multiple specificities are tracked together under the umbrella of a single barcode. On the other hand, we have noted a number of barcodes that are unique in rhesus NK cells and not found in other linages or are detected at much higher frequency in NK cells compared with other cell types.[41,42] It is probable that these have arisen during NK cell development *in vivo* via a clonal expansion from one or a few NK cells, representing true clonal or oligoclonal NK cell expansions, potentially with unique self-renewal properties and linked to adaptive characteristics of subpopulations of NK cells. Notably, barcodes statistically categorized as "pre-expanded *in vivo*" in NK cells also showed considerable capacity to expand *in vitro* when cultured with irradiated feeders (Figure 4).

Due to this experimental system, individual barcodes may mark from one cell to tens of thousands of individual NK cells used to initiate the *in vitro* cultures. Therefore, results showing maintenance of the majority of barcodes could be consistent with a smaller proportion of individual NK cells having proliferative potential. Future studies will address this quantitatively. In addition, it is possible that the observed homogeneity of barcode behavior may be partly attributed to averaging of multiple NK cells.

Expression of KIR, which have been reported to be stably expressed on NK cells,[54] can also help illuminate the categorization of barcodes. NK cells with a given barcode that also uniformly do or do not express KIR3DL01 provide persuasive evidence that these clones were derived from a single NK cell or NK cell progenitor that had fixed its KIR expression. On the other hand, barcodes detected in both $KIR3DL01^+$ and $KIR3DL01^-$ populations may represent the aforementioned pools of mixed NK specificities from a given HSPC. All three categories of barcodes, with respect to KIR3DL01 expression, showed proliferation when cultured *in vitro* with irradiated feeder cells. Therefore, where evidence implied that barcodes were truly equivalent to NK cell clones, these clones appeared to expand using these *ex vivo* expansion protocols. However, even in the case of these KIR-restricted NK cell clones, which developed *in vivo* since transplantation 41 to 76 months previously, there was opportunity since clonal origination for cells to acquire or lose other NK cell receptors to form subclones. Like T cell clones, clonal subsets may have

frequency in either $CD56^+$ or $CD16^+$ NK populations. (A) An example of rhesus macaque $NKG2^+$ $CD3^-$ NK cell expression of CD56 and CD16 before and after culture with irradiated LCL feeder cells and IL-2. (B) Contribution of clones categorized initially as CD56 NK-cell-biased or CD16 NK-cell-biased to the overall NK cell repertoire throughout *in vitro* culture (sum of frequencies of barcodes in each category at the time points analyzed). White areas represent clones lacking bias or having insufficient sample size to statistically classify. (C) NK cell subsets were sorted again after culture of the bulk NK cell population and profiled by barcode PCR and sequencing. Contributions of clones initially classified as CD56 NK-cell-biased or CD16 NK-cell-biased to the repertoire of sorted subsets after culture are shown (legend as in B). DP, double-positive $CD16^+$ $CD56^+$; DN, double-negative $CD16^-$ $CD56^-$, while CD16 and CD56 represent sorted single positive populations. Cultures depicted in (A)–(C) were stimulated with the indicated feeder cell line only initially, except for ZH19 cultures in (B), which were also restimulated after approximately 1 week.

developed with epigenetic, transcriptional, or metabolic heterogeneity with varied behaviors, seen only in aggregate/average in our experiments.

When following barcoded macaques over extended periods, many expanded NK cell clones were shown to persist at high frequency for many months.[41] These expanded and persistent clones may therefore represent long-lived memory-like/adaptive/trained NK cells[44,47,48] and/or be continually stimulated *in vivo*, possibly via stimulation by chronic pathogen infection.[41] Interestingly, new clonal expansions were observed after CMV infection of CMV-naive macaques,[43] perhaps akin to accumulation of NKG2C$^+$ (KLRC2$^+$) memory-like NK cells associated with CMV infection in humans. In this context, it is notable that clones categorized as "pre-expanded in *vivo*," representing putative memory-like NK cells, maintained considerable proliferative capacity when stimulated in the *in vitro* expansion culture systems, although less efficiently than barcoded NK cells that were not designated as expanded (Figure 4). The slight diminishment of *ex vivo* growth capacity could reflect a lessened potential or a greater tendency toward exhaustion after prior *in vivo* proliferation. While others have devised strategies for the specific amplification of memory-like NK cells to harness their unique features (e.g., Liu et al.[55]), it is striking that putative memory-like cells continue to constitute a significant fraction of the bulk cell NK cell repertoire contained in expansion cultures stimulated with irradiated feeder cells.

Expansion of a diverse repertoire of clones, including those preponderant initially in either CD56^{bright}- or CD56^{dim}-like NK cell populations (Figure 6), is noteworthy given the propensity of IL-2 or IL-15 to selectively expand CD56^{bright} NK cells.[12] Also, changes to the clonal repertoire were similar whether NK cells were stimulated with irradiated EBV-LCL or K562 cells expressing 4-1BBL and IL-21, two frequently used feeder cell populations used in expansion protocols (Figure 3). This may indicate that signals that induce proliferation are conserved between both systems and is consistent with findings that human NK cells expanded in parallel with either of these two feeder cell lines are highly similar, showing only a few differentially expressed genes when queried by whole-transcriptome sequencing.[22,23]

The results presented here may have significant implications for adoptive immunotherapy using expanded NK cells. Notably, the proliferation of a diverse repertoire of clones suggests that the expanded product may retain many of the initial receptor combinations that have unique potential to kill tumor targets and may be important for maintaining the full spectrum of NK reactivity and functionality. In this way, expanded NK cell populations used for treatment that have an obvious advantage in cell numbers may not be disadvantaged by having a less diverse repertoire compared with short-term cytokine-stimulated cells. Importantly, the observation that cultures stimulated with feeder cells showed a significant proportion of the expanded product contained clones representing putative memory-like NK cells suggests that these populations could make long-term functional contributions to the activity of the infused *ex vivo* expanded NK cell product. Analogous to clinical results with expanded viral-reactive T cells and CAR T cells, where *in vivo* persistence correlates with durable anti-viral activity and remissions of leukemia, respectively,[56,57] expanded NK cell products that maintain a rich population of memory-like cells may likewise be advantageous for maintaining clinical efficacy. This remains an area of active investigation.[55]

MATERIALS AND METHODS

Cell lines

SMI-LCL is an EBV-transformed B cell LCL previously described.[58,59] The clone 46 K562 cell line was retrovirally modified to express 4-1BBL and membrane-bound IL-21 and has been described.[22] Both lines were cultured in RPMI medium containing 2 mM L-glutamine supplemented with 10% fetal bovine serum.

Transplanted rhesus macaques

Animal studies were carried out on protocols approved by the National Heart, Lung, and Blood Institute Animal Care and Use Committee. Rhesus macaques previously received autologous hematopoietic stem cell transplants after total-body irradiation with mobilized peripheral blood CD34$^+$ cells transduced with lentiviral libraries encoding CopGFP and a high-diversity genetic barcode.[41,42] At the time of the experiments shown here, animals with identifiers ZK22, ZJ31, ZH19, and ZG66 were 41, 51, 74, and 76 months post-transplant, respectively, and exhibited approximately 43%, 50%, 7.4%, and 32% GFP$^+$ cells, respectively, within the peripheral blood mononuclear cell (PBMC) population. These animals did not undergo prior antibody-mediated depletion of NK cells.[41]

Isolation of NK cells

PBMCs from rhesus macaque blood samples were isolated with lymphocyte separation medium (MP Biomedicals, Irvine, CA, USA). Cells were stained with combinations of antibodies recognizing NKG2 (Z199) from Beckman Coulter (Brea, CA, USA); CD56 (NCAM16.2 or B159), CD20 (L27), and CD3 (SP34-2) from BD Biosciences (Franklin Lakes, NJ, USA); CD3 (10D12) and KIR (NKVFS1) from Miltenyi Biotec (Bergisch Gladbach, Germany); CD16 (3G8) and CD14 (M5E2) from BioLegend (San Diego, CA, USA); and CD14 (TuK4) from Invitrogen Thermo Fisher Scientific (Waltham, MA, USA) before flow cytometric sorting on a FACSAria II (BD Biosciences). Macaque NK cells were sorted based on the phenotype NKG2$^+$ CD3$^-$ CD20$^-$ CD14$^-$, and NK cell subsets were sorted defined by CD56, CD16, and NKVFS1 reactivity. CD14$^+$ monocytes were concurrently isolated.

Ex vivo expansion of NK cells

Co-cultures were initiated by combining 2–6 $\times$ 10^5 isolated macaque NK cells with gamma-irradiated (100 Gy) LCL cells at a 10:1 LCL:NK cell ratio in X-VIVO 20 medium (Lonza, Basel, Switzerland) supplemented with 10% heat-inactivated allogeneic rhesus macaque serum, 2 mM GlutaMAX (Thermo Fisher Scientific), and 500 IU/mL human IL-2 (teceleukin, Roche, Basel, Switzerland). Co-cultures with irradiated 4-1BBL$^+$ IL-21$^+$ K562 feeder cells were initiated at a 2:1 K562

cell:NK cell ratio (reflecting established protocols and differences in cell size) using the same medium and IL-2 concentration. After an initial culture of 5–7 days, cells were subcultured every 2–3 days, refreshing medium and IL-2. Cell numbers were monitored throughout by trypan blue staining and light microscopy and used to calculate the cumulative fold change in overall NK cell numbers. Some cultures had feeder cells present only initially, while others, as indicated, were restimulated approximately weekly by the addition of irradiated feeder cells at 2.5:1 LCL:NK cell or 1:1 K562 cell:NK cell ratios. Cells were sampled initially and periodically throughout culture and frozen as pellets for subsequent DNA barcode analysis by PCR. After 14–24 days culture, cells were stained and sorted to obtain NKG2$^+$ CD3$^-$ NK cell subsets defined by CD56 and CD16.

Barcode retrieval

Integrated lentiviral barcode sequences were amplified and sequenced as previously described.[41] Briefly, DNA was isolated using DNeasy blood and tissue kit (Qiagen, Hilden, Germany) or cells lysed with Direct PCR lysis reagent (Viagen Biotech, Los Angeles, CA, USA) with added 1 mg/mL proteinase K (Qiagen) and 2 mg/mL RNAse A (Qiagen). Cell lysate from a defined number of cells or 200–500 ng DNA was PCR amplified using primers spanning the barcode cassette, gel purified, and sequenced on an Illumina HiSeq 2500 or 3000. Initial processing of sequencing data was performed as described[41,43] but omitting a threshold of unique sequence reads per barcode for initial inclusion into the dataset. Some analyses were performed using the barcodetrackR package.[60] One clone in blood of animal ZH19, present in bulk samples but detected much less in GFP$^+$ sorted samples, was excluded from certain analyses containing groups that differed in sorting status (e.g., Figures 3A–3C and S2A).

Barcode frequency analysis and comparison between cell populations

Barcodes with frequencies below the equivalent of 1 cell amid the estimated number of GFP$^+$ cells initially sampled by PCR were excluded from consideration. To facilitate statistical comparison of barcode abundance between isolated cell populations, barcode sequence read frequencies were used to impute the number of cells among the isolated cell population that contained a given barcode as follows:

$$n_{barcode} = \left(\frac{sequence\ reads_{barcode}}{sequence\ reads_{all\ barcodes}} \right) \times number\ of\ GFP^+\ cells\ sampled\ by\ PCR$$

When comparing two isolated cell populations, these imputed estimates of numbers of isolated cells bearing a given barcode were compared by chi-squared test or used to construct confidence intervals for the ratio of barcode proportions between populations using the adjusted log method[61] based on Katz et al.[62] This facilitated classification of barcode clones that were below a chi-squared p value threshold or exhibited confidence intervals outside a defined fold-difference threshold. These comparisons and statistics are explained in more detail in the supplemental methods, and R code to perform the analyses shown herein is available upon request.

DATA AVAILABILITY

Data are available from the authors upon request.

SUPPLEMENTAL INFORMATION

Supplemental information can be found online at https://doi.org/10.1016/j.omto.2022.12.006.

ACKNOWLEDGMENTS

We thank Stefan Cordes and Xin Tian for advice about statistical testing; Xing Fan for creating the graphical abstract art; Muna Igboko for reviewing R code; Keyvan Keyvanfar for flow cytometric cell sorting; Richard Lozano for experimental assistance; Annie Liang and Lauren Truitt for sequence data processing; the NHLBI DNA Sequencing and Genomics Core; and the NHLBI Non-human Primate Program for care of the animals. This work was supported by the NHLBI Division of Intramural Research and by the commissioned corps of the United States Public Health Service.

AUTHOR CONTRIBUTIONS

Conceptualization, C.E.D., D.S.J.A., C.W., J.K.D.-M., and R.W.C.; investigation, C.W., D.S.J.A., and M.C.; software, D.S.J.A. and R.D.M.; formal analysis, D.S.J.A. and R.D.M.; visualization, D.S.J.A.; resources, K.R.; writing – original draft, D.S.J.A.; writing – review & editing, C.E.D., R.W.C., D.S.J.A., and C.W.; supervision, C.E.D. and R.W.C.

DECLARATION OF INTERESTS

K.R. and The University of Texas MD Anderson Cancer Center have an institutional financial conflict of interest with Takeda Pharmaceutical and with Affimed GmbH. K.R. is a member of the Scientific Advisory Boards for GemoAb, AvengeBio, Virogin Biotech, GSK, Caribou Biosciences, Navan Technologies, and Bayer. J.K.D.-M. is an employee of Wugen.

REFERENCES

1. Shimasaki, N., Jain, A., and Campana, D. (2020). NK cells for cancer immunotherapy. Nat. Rev. Drug Discov. *19*, 200–218.

2. Childs, R.W., and Carlsten, M. (2015). Therapeutic approaches to enhance natural killer cell cytotoxicity against cancer: the force awakens. Nat. Rev. Drug Discov. *14*, 487–498.

3. Miller, J.S., Soignier, Y., Panoskaltsis-Mortari, A., McNearney, S.A., Yun, G.H., Fautsch, S.K., McKenna, D., Le, C., Defor, T.E., Burns, L.J., et al. (2005). Successful adoptive transfer and in vivo expansion of human haploidentical NK cells in patients with cancer. Blood *105*, 3051–3057.

4. Cooley, S., He, F., Bachanova, V., Vercellotti, G.M., DeFor, T.E., Curtsinger, J.M., Robertson, P., Grzywacz, B., Conlon, K.C., Waldmann, T.A., et al. (2019). First-in-human trial of rhIL-15 and haploidentical natural killer cell therapy for advanced acute myeloid leukemia. Blood Adv. *3*, 1970–1980.

5. Bachanova, V., Cooley, S., Defor, T.E., Verneris, M.R., Zhang, B., McKenna, D.H., Curtsinger, J., Panoskaltsis-Mortari, A., Lewis, D., Hippen, K., et al. (2014). Clearance of acute myeloid leukemia by haploidentical natural killer cells is improved using IL-2 diphtheria toxin fusion protein. Blood *123*, 3855–3863.

6. Björklund, A.T., Carlsten, M., Sohlberg, E., Liu, L.L., Clancy, T., Karimi, M., Cooley, S., Miller, J.S., Klimkowska, M., Schaffer, M., et al. (2018). Complete remission with reduction of high-risk clones following haploidentical NK-cell therapy against MDS and AML. Clin. Cancer Res. *24*, 1834–1844.

7. Romee, R., Rosario, M., Berrien-Elliott, M.M., Wagner, J.A., Jewell, B.A., Schappe, T., Leong, J.W., Abdel-Latif, S., Schneider, S.E., Willey, S., et al. (2016). Cytokine-induced memory-like natural killer cells exhibit enhanced responses against myeloid leukemia. Sci. Transl. Med. *8*, 357ra123.

8. Federico, S.M., McCarville, M.B., Shulkin, B.L., Sondel, P.M., Hank, J.A., Hutson, P., Meagher, M., Shafer, A., Ng, C.Y., Leung, W., et al. (2017). A pilot trial of humanized anti-GD2 monoclonal antibody (hu14.18K322A) with chemotherapy and natural killer cells in children with recurrent/refractory neuroblastoma. Clin. Cancer Res. *23*, 6441–6449.

9. Modak, S., Le Luduec, J.B., Cheung, I.Y., Goldman, D.A., Ostrovnaya, I., Doubrovina, E., Basu, E., Kushner, B.H., Kramer, K., Roberts, S.S., et al. (2018). Adoptive immunotherapy with haploidentical natural killer cells and Anti-GD2 monoclonal antibody m3F8 for resistant neuroblastoma: results of a phase I study. Oncoimmunology *7*, e1461305.

10. Bachanova, V., Sarhan, D., DeFor, T.E., Cooley, S., Panoskaltsis-Mortari, A., Blazar, B.R., Curtsinger, J.M., Burns, L., Weisdorf, D.J., and Miller, J.S. (2018). Haploidentical natural killer cells induce remissions in non-Hodgkin lymphoma patients with low levels of immune-suppressor cells. Cancer Immunol. Immunother. *67*, 483–494.

11. Robertson, M.J., Manley, T.J., Donahue, C., Levine, H., and Ritz, J. (1993). Costimulatory signals are required for optimal proliferation of human natural killer cells. J. Immunol. *150*, 1705–1714.

12. Carson, W.E., Giri, J.G., Lindemann, M.J., Linett, M.L., Ahdieh, M., Paxton, R., Anderson, D., Eisenmann, J., Grabstein, K., and Caligiuri, M.A. (1994). Interleukin (IL) 15 is a novel cytokine that activates human natural killer cells via components of the IL-2 receptor. J. Exp. Med. *180*, 1395–1403.

13. Fujisaki, H., Kakuda, H., Shimasaki, N., Imai, C., Ma, J., Lockey, T., Eldridge, P., Leung, W.H., and Campana, D. (2009). Expansion of highly cytotoxic human natural killer cells for cancer cell therapy. Cancer Res. *69*, 4010–4017.

14. Hercend, T., Meuer, S., Reinherz, E.L., Schlossman, S.F., and Ritz, J. (1982). Generation of a cloned NK cell line derived from the "null cell" fraction of human peripheral blood. J. Immunol. *129*, 1299–1305.

15. London, L., Perussia, B., and Trinchieri, G. (1986). Induction of proliferation in vitro of resting human natural killer cells: IL 2 induces into cell cycle most peripheral blood NK cells, but only a minor subset of low density T cells. J. Immunol. *137*, 3845–3854.

16. Perussia, B., Ramoni, C., Anegon, I., Cuturi, M.C., Faust, J., and Trinchieri, G. (1987). Preferential proliferation of natural killer cells among peripheral blood mononuclear cells cocultured with B lymphoblastoid cell lines. Nat. Immun. Cell Growth Regul. *6*, 171–188.

17. Berg, M., Lundqvist, A., McCoy, P., Jr., Samsel, L., Fan, Y., Tawab, A., and Childs, R. (2009). Clinical-grade ex vivo-expanded human natural killer cells up-regulate activating receptors and death receptor ligands and have enhanced cytolytic activity against tumor cells. Cytotherapy *11*, 341–355.

18. Lundqvist, A., Berg, M., Smith, A., and Childs, R.W. (2011). Bortezomib treatment to potentiate the anti-tumor immunity of ex-vivo expanded adoptively infused autologous natural killer cells. J. Cancer *2*, 383–385.

19. Lundqvist, A., Yokoyama, H., Smith, A., Berg, M., and Childs, R. (2009). Bortezomib treatment and regulatory T-cell depletion enhance the antitumor effects of adoptively infused NK cells. Blood *113*, 6120–6127.

20. Imai, C., Iwamoto, S., and Campana, D. (2005). Genetic modification of primary natural killer cells overcomes inhibitory signals and induces specific killing of leukemic cells. Blood *106*, 376–383.

21. Denman, C.J., Senyukov, V.V., Somanchi, S.S., Phatarpekar, P.V., Kopp, L.M., Johnson, J.L., Singh, H., Hurton, L., Maiti, S.N., Huls, M.H., et al. (2012). Membrane-bound IL-21 promotes sustained ex vivo proliferation of human natural killer cells. PLoS One *7*, e30264.

22. Liu, E., Ang, S.O.T., Kerbauy, L., Basar, R., Kaur, I., Kaplan, M., Li, L., Tong, Y., Daher, M., Ensley, E.L., et al. (2021). GMP-compliant universal antigen presenting cells (uAPC) promote the metabolic fitness and antitumor activity of armored cord blood CAR-NK cells. Front. Immunol. *12*, 626098.

23. Levy, E.R., Clara, J.A., Reger, R.N., Allan, D.S.J., and Childs, R.W. (2021). RNA-seq analysis reveals CCR5 as a key target for CRISPR gene editing to regulate in vivo NK cell trafficking. Cancers (Basel) *13*, 872.

24. Ciurea, S.O., Schafer, J.R., Bassett, R., Denman, C.J., Cao, K., Willis, D., Rondon, G., Chen, J., Soebbing, D., Kaur, I., et al. (2017). Phase 1 clinical trial using mbIL21 ex vivo-expanded donor-derived NK cells after haploidentical transplantation. Blood *130*, 1857–1868.

25. Mani, R., Rajgolikar, G., Nunes, J., Zapolnik, K., Wasmuth, R., Mo, X., Byrd, J.C., Lee, D.A., Muthusamy, N., and Vasu, S. (2020). Fc-engineered anti-CD33 monoclonal antibody potentiates cytotoxicity of membrane-bound interleukin-21 expanded natural killer cells in acute myeloid leukemia. Cytotherapy *22*, 369–376.

26. Zhao, X.Y., Jiang, Q., Jiang, H., Hu, L.J., Zhao, T., Yu, X.X., and Huang, X.J. (2020). Expanded clinical-grade membrane-bound IL-21/4-1BBL NK cell products exhibit activity against acute myeloid leukemia in vivo. Eur. J. Immunol. *50*, 1374–1385.

27. Gómez García, L.M., Escudero, A., Mestre, C., Fuster Soler, J.L., Martínez, A.P., Vagace Valero, J.M., Vela, M., Ruz, B., Navarro, A., Fernández, L., et al. (2021). Phase 2 clinical trial of infusing haploidentical K562-mb15-41BBL-Activated and expanded natural killer cells as consolidation therapy for pediatric acute myeloblastic leukemia. Clin. Lymphoma, Myeloma & Leukemia *21*, 328–337.e1.

28. Khatua, S., Cooper, L.J.N., Sandberg, D.I., Ketonen, L., Johnson, J.M., Rytting, M.E., Liu, D.D., Meador, H., Trikha, P., Nakkula, R.J., et al. (2020). Phase I study of intraventricular infusions of autologous ex vivo expanded NK cells in children with recurrent medulloblastoma and ependymoma. Neuro. Oncol. *22*, 1214–1225.

29. Szmania, S., Lapteva, N., Garg, T., Greenway, A., Lingo, J., Nair, B., Stone, K., Woods, E., Khan, J., Stivers, J., et al. (2015). Ex vivo-expanded natural killer cells demonstrate robust proliferation in vivo in high-risk relapsed multiple myeloma patients. J. Immunother. *38*, 24–36.

30. Leivas, A., Perez-Martinez, A., Blanchard, M.J., Martín-Clavero, E., Fernández, L., Lahuerta, J.J., and Martinez-Lopez, J. (2016). Novel treatment strategy with autologous activated and expanded natural killer cells plus anti-myeloma drugs for multiple myeloma. Oncoimmunology *5*, e1250051.

31. Shah, N.N., Baird, K., Delbrook, C.P., Fleisher, T.A., Kohler, M.E., Rampertaap, S., Lemberg, K., Hurley, C.K., Kleiner, D.E., Merchant, M.S., et al. (2015). Acute GVHD in patients receiving IL-15/4-1BBL activated NK cells following T-cell-depleted stem cell transplantation. Blood *125*, 784–792.

32. Liu, E., Tong, Y., Dotti, G., Shaim, H., Savoldo, B., Mukherjee, M., Orange, J., Wan, X., Lu, X., Reynolds, A., et al. (2018). Cord blood NK cells engineered to express IL-15 and a CD19-targeted CAR show long-term persistence and potent antitumor activity. Leukemia *32*, 520–531.

33. Liu, E., Marin, D., Banerjee, P., Macapinlac, H.A., Thompson, P., Basar, R., Nassif Kerbauy, L., Overman, B., Thall, P., Kaplan, M., et al. (2020). Use of CAR-transduced natural killer cells in CD19-positive lymphoid tumors. N. Engl. J. Med. *382*, 545–553.

34. Allan, D.S.J., Chakraborty, M., Waller, G.C., Hochman, M.J., Poolcharoen, A., Reger, R.N., and Childs, R.W. (2021). Systematic improvements in lentiviral transduction of primary human natural killer cells undergoing ex vivo expansion. Mol. Ther. Methods Clin. Dev. *20*, 559–571.

35. Chanswangphuwana, C., Allan, D.S.J., Chakraborty, M., Reger, R.N., and Childs, R.W. (2021). Augmentation of NK cell proliferation and anti-tumor immunity by transgenic expression of receptors for EPO or TPO. Mol. Ther. *29*, 47–59.

36. Manser, A.R., Weinhold, S., and Uhrberg, M. (2015). Human KIR repertoires: shaped by genetic diversity and evolution. Immunol. Rev. *267*, 178–196.

37. Strunz, B., Hengst, J., Deterding, K., Manns, M.P., Cornberg, M., Ljunggren, H.G., Wedemeyer, H., and Björkström, N.K. (2018). Chronic hepatitis C virus infection irreversibly impacts human natural killer cell repertoire diversity. Nat. Commun. *9*, 2275.

38. Horowitz, A., Strauss-Albee, D.M., Leipold, M., Kubo, J., Nemat-Gorgani, N., Dogan, O.C., Dekker, C.L., Mackey, S., Maecker, H., Swan, G.E., et al. (2013). Genetic and environmental determinants of human NK cell diversity revealed by mass cytometry. Sci. Transl. Med. *5*, 208ra145.

39. Poschke, I.C., Hassel, J.C., Rodriguez-Ehrenfried, A., Lindner, K.A.M., Heras-Murillo, I., Appel, L.M., Lehmann, J., Lövgren, T., Wickström, S.L., Lauenstein, C., et al. (2020). The outcome of ex vivo TIL expansion is highly influenced by spatial

heterogeneity of the tumor T-cell repertoire and differences in intrinsic in vitro growth capacity between T-cell clones. Clin. Cancer Res. *26*, 4289–4301.

40. Koning, D., Costa, A.I., Hasrat, R., Grady, B.P.X., Spijkers, S., Nanlohy, N., Keşmir, C., and van Baarle, D. (2014). In vitro expansion of antigen-specific CD8(+) T cells distorts the T-cell repertoire. J. Immunol. Methods *405*, 199–203.

41. Wu, C., Espinoza, D.A., Koelle, S.J., Yang, D., Truitt, L., Schlums, H., Lafont, B.A., Davidson-Moncada, J.K., Lu, R., Kaur, A., et al. (2018). Clonal expansion and compartmentalized maintenance of rhesus macaque NK cell subsets. Sci. Immunol. *3*, eaat9781.

42. Wu, C., Li, B., Lu, R., Koelle, S.J., Yang, Y., Jares, A., Krouse, A.E., Metzger, M., Liang, F., Loré, K., et al. (2014). Clonal tracking of rhesus macaque hematopoiesis highlights a distinct lineage origin for natural killer cells. Cell Stem Cell *14*, 486–499.

43. Truitt, L.L., Yang, D., Espinoza, D.A., Fan, X., Ram, D.R., Moström, M.J., Tran, D., Sprehe, L.M., Reeves, R.K., Donahue, R.E., et al. (2019). Impact of CMV infection on natural killer cell clonal repertoire in CMV-naive rhesus macaques. Front. Immunol. *10*, 2381.

44. Mujal, A.M., Delconte, R.B., and Sun, J.C. (2021). Natural killer cells: from innate to adaptive features. Annu. Rev. Immunol. *39*, 417–447.

45. Chiffelle, J., Genolet, R., Perez, M.A., Coukos, G., Zoete, V., and Harari, A. (2020). T-cell repertoire analysis and metrics of diversity and clonality. Curr. Opin. Biotechnol. *65*, 284–295.

46. Patel, A.A., Zhang, Y., Fullerton, J.N., Boelen, L., Rongvaux, A., Maini, A.A., Bigley, V., Flavell, R.A., Gilroy, D.W., Asquith, B., et al. (2017). The fate and lifespan of human monocyte subsets in steady state and systemic inflammation. J. Exp. Med. *214*, 1913–1923.

47. Schlums, H., Cichocki, F., Tesi, B., Theorell, J., Beziat, V., Holmes, T.D., Han, H., Chiang, S.C.C., Foley, B., Mattsson, K., et al. (2015). Cytomegalovirus infection drives adaptive epigenetic diversification of NK cells with altered signaling and effector function. Immunity *42*, 443–456.

48. Netea, M.G., Domínguez-Andrés, J., Barreiro, L.B., Chavakis, T., Divangahi, M., Fuchs, E., Joosten, L.A.B., van der Meer, J.W.M., Mhlanga, M.M., Mulder, W.J.M., et al. (2020). Defining trained immunity and its role in health and disease. Nat. Rev. Immunol. *20*, 375–388.

49. Schafer, J.L., Colantonio, A.D., Neidermyer, W.J., Dudley, D.M., Connole, M., O'Connor, D.H., and Evans, D.T. (2014). KIR3DL01 recognition of Bw4 ligands in the rhesus macaque: maintenance of Bw4 specificity since the divergence of apes and Old World monkeys. J. Immunol. *192*, 1907–1917.

50. Older Aguilar, A.M., Guethlein, L.A., Hermes, M., Walter, L., and Parham, P. (2011). Rhesus macaque KIR bind human MHC class I with broad specificity and recognize HLA-C more effectively than HLA-A and HLA-B. Immunogenetics *63*, 577–585.

51. Leijonhufvud, C., Reger, R., Segerberg, F., Theorell, J., Schlums, H., Bryceson, Y.T., Childs, R.W., and Carlsten, M. (2021). LIR-1 educates expanded human NK cells and defines a unique antitumor NK cell subset with potent antibody-dependent cellular cytotoxicity. Clin. Transl. Immunol. *10*, e1346.

52. Webster, R.L., and Johnson, R.P. (2005). Delineation of multiple subpopulations of natural killer cells in rhesus macaques. Immunology *115*, 206–214.

53. Davidson-Moncada, J.K., Childs, R., Dunbar, C.E., Reger, R., Kotecha, R., Berg, M., and Wu, C. (2013). Rhesus macaque NK cells expanded ex vivo undergo similar phenotypic and functional changes observed with expanded human NK cells providing an excellent model to optimize adoptive NK cell transfer. Blood *122*, 2028.

54. Cichocki, F., Miller, J.S., and Anderson, S.K. (2011). Killer immunoglobulin-like receptor transcriptional regulation: a fascinating dance of multiple promoters. J. Innate Immun. *3*, 242–248.

55. Liu, L.L., Béziat, V., Oei, V.Y.S., Pfefferle, A., Schaffer, M., Lehmann, S., Hellström-Lindberg, E., Söderhäll, S., Heyman, M., Grandér, D., and Malmberg, K.J. (2017). Ex vivo expanded adaptive NK cells effectively kill primary acute lymphoblastic leukemia cells. Cancer Immunol. Res. *5*, 654–665.

56. Keller, M.D., and Bollard, C.M. (2020). Virus-specific T-cell therapies for patients with primary immune deficiency. Blood *135*, 620–628.

57. Gupta, A., and Gill, S. (2021). CAR-T cell persistence in the treatment of leukemia and lymphoma. Leuk. Lymphoma *62*, 2587–2599.

58. Childs, R.W., and Berg, M. (2013). Bringing natural killer cells to the clinic: ex vivo manipulation. Hematol. Am. Soc. Hematol. Educ. Program *2013*, 234–246.

59. Carlsten, M., Levy, E., Karambelkar, A., Li, L., Reger, R., Berg, M., Peshwa, M.V., and Childs, R.W. (2016). Efficient mRNA-based genetic engineering of human NK cells with high-affinity CD16 and CCR7 augments rituximab-induced ADCC against lymphoma and targets NK cell migration toward the lymph node-associated chemokine CCL19. Front. Immunol. *7*, 105.

60. Espinoza, D.A., Mortlock, R.D., Koelle, S.J., Wu, C., and Dunbar, C.E. (2021). Interrogation of clonal tracking data using barcodetrackR. Nat. Comput. Sci. *1*, 280–289.

61. Fagerland, M.W., Lydersen, S., and Laake, P. (2015). Recommended confidence intervals for two independent binomial proportions. Stat. Methods Med. Res. *24*, 224–254.

62. Katz, D., Baptista, J., Azen, S.P., and Pike, M.C. (1978). Obtaining confidence intervals for risk ratio in cohort studies. Biometrics *34*, 469–474.